Int J Burn Trauma 2022;12(1):28-34
www.IJBT.org /ISSN:2160-2026/IJBT0139226

Original Article

Application of berberine-loaded albumin nanoparticles in infections of traumatic wounds

Zhenqiang Liu[1*], Yanchao Liu[2*], Ting Fang[3], Jianhua Xia[4], Ning Ma[5], Yanhong Wang[1]

[1]Heilongjiang University of Chinese Medicine, Heilongjiang Province, No. 24 Heping Road, Harbin 150040, Heilongjiang Province, China; [2]Department of Clinical Pharmacy, Shanghai General Hospital, School of Medicine, Shanghai Jiaotong University, Shanghai 201620, China; [3]Department of Pharmacology, Shanghai Tenth People's Hospital, Tongji University School of Medicine, 1239 Siping Road, Shanghai 200092, China; [4]Department of Anesthesiology, Shanghai Pudong New Area People's Hospital, 490 South Chuanhuan Road, Shanghai 201299, China; [5]Department of Clinical Laboratory, 905th Hospital of PLA, Shanghai 200052, China. [*]Equal contributors.

Received September 17, 2021; Accepted January 20, 2022; Epub February 15, 2022; Published February 28, 2022

Abstract: In recent years, the morbidity of infections in traumatic wounds has been on the increase. There are not many kinds of drugs for clinical treatment of infections, and their efficacy and safety are limited. Plant antimicrobial drugs are increasingly popular in mainstream medicine due to the challenges of traditional antibiotics abuse. Berberine has a scavenging effect on infections, however, berberine was restricted from using as a drug preparation with poor stability and bioavailability. Due to the low toxicity of nanoparticles, the green-synthetic, size-controlled approach of nanoparticles has been paid more attention. Therefore, based on the intermolecular disulfide bond network platform built earlier, we designed and developed a strategy to assemble molecular bovine serum albumin into large-sized nanostructures through the reconstructed intermolecular disulfide bond and hydrophobic interaction, and berberine with poor water solubility was encapsulated in it. Nanoassembly with bovine serum albumin increased biostability of berberine and significantly improved its activity against Staphylococcus Aureus (*S.aureus*) activity, which gives some new insights into the preparation and development of anti-infectives for Chinese medicine.

Keywords: Infections, berberine, albumin nanoparticles, green-synthetic

Introduction

Tissue fragments, dirt, hair and necrotic tissue are common in traumatic wounds. The aggravation of inflammatory reaction and even secondary infection, and then delay the wound repair can be involved [1]. When individual immunity is impaired under such conditions, patients may become vulnerable to microorganisms, resulting in an increase in the incidence of infections every year [2-4]. Therefore, wound infection is the most common and influential serious problem after traumatic injury. It will cause sepsis, amputation and other adverse complications, and even lead to death [5, 6]. In 2017, a systematic evaluation and meta-analysis reported that the global chronic wound infection rate was 78.2%, and most of the pathogens of chronic wound infection were Staphylococcus Aureus and Pseudomonas Aeruginosa [7].

Due to the longer cycle and higher risk of new drug development, it has become a major problem that how to make full use of existing resources to improve the efficacy of anti-infection drugs. Medicinal plants are one of the potential sources of antibiotics [8-10]. Plant antimicrobial drugs are more and more popular in mainstream medicine due to the challenges of traditional antibiotics abuse.

Berberine (BBR), as a natural isoquinoline alkaloid, is derived from Chinese medicinal herbs, especially Berberis vulgaris. It exhibits many biological effects, including anti-viral, antimicrobial, anti-diarrhea, anti-inflammatory and anti-cancer effects [11, 12]. But its poor aqueous solubility, slight absorption, low bioavailability and selectivity limit berberine therapeutic use [11, 13-15]. To overcome these limitations, nanotechnology has been considered as main strategy [16, 17].

In recent years, nano-antibiotics not only improve the therapeutic efficiency, but also reduce the toxicity of some drugs [18]. It has become a research focus that using natural biomass as reactants or constructions to build functional nanostructures. Albumin has attracted increasing attention since the FDA approved the marketing of albumin-bound paclitaxel nanoparticles in 2005. As a biological carrier, albumin has the characteristics of biocompatible and non-toxic, and as an endogenous substance, albumin can prolong the circulation time of drugs in vivo [19, 20]. We have designed and used a safe nanocarrier based on Bovine serum albumin (BSA), which is a natural and biodegradable material. The study uses self-assembly nanotechnology to meliorate the biological activity of BBR. The self-assembled nanomedicines are easy to synthesize and possess high drug-loading capacity, in other words, they could achieve high and stable delivery of drugs without any other carrier [21, 22].

For this purpose, based on the previously built intermolecular disulfide bond network platform, we assemble molecular BSA into large-sized nanostructures, which uses the reconstructed intermolecular disulfide bond and hydrophobic interaction. Then berberine, a kind of low water-solubility drug, is stable in BSA structure through hydrophobic interaction and hydrogen bonding to increase solubility. They could be used to combat microbe resistance and enhance the efficacy of antibiotics.

Materials and methods

Reagents

BBR and Vancomycin (VA) were purchased from Meilunbio. Sodium dodecyl sulfate (SDS), dithiothreitol (DTT), Urea, and 2-morpholinoethanesulfonic acid (MES) were purchased from Aladdin. BSA was purchased from Sigma-Aldrich. RPMI 1640 medium and phosphate buffered solution (PBS) were purchased from Hyclone. Luria-Bertani (LB) medium was purchased from Sangon Biotech.

Strains

All strains were maintained on LB agar plates and cultured in LB liquid medium. For all experiments, the colonies were washed in PBS three times before use.

Preparation of BBR-NP

The intramolecular disulfide bonds and hydrophobic forces of BSA (40 mg/mL) were eliminated by treatment of SDS (2% [wt/vol]) and DTT (0.15% [wt/vol]) regents, resulting in liberation of free thiol. As we have previously reported, the protein was denatured by heating to release free thiol, the reduced BSA (rBSA) was obtained by heating the processed BSA to 90°C for 2 h [23, 24]. rBSA was dissolved in PBS (0.0067M PO_4) and nanoparticles (BBR-NP) were prepared by adding BBR in magnetic stirrer (the proportion between BBR and BSA is w/w 1:1, 1:2, 1:5, 1:10). BSA nanoparticles (BSA-NP) assembly occurred with the same method. The free drugs and additives were removed by dialysis. Finally, the BBR-NP was characterized after ultrafiltration (MW10 KD), and the best mass ratio was selected by the results.

Characterization of BBR-NP

The particle size and zeta potential of BSA-NP, BBR-NP were determined by dynamic light scattering (DLS) (Zetasizer Nano ZS, ZEN3690, Malvern). The preparation scheme was selected by the particle size and distribution of BBR-NP with different feeding ratios. All measurements were carried out in triplicates. The morphology of nanoparticle was observed by transmission electron microscope (TEM) (Tecnai-12Bio-Twin, FEI, Netherlands). BBR-NP was prepared and dialyzed for 48 h (MW14000), then free drugs, SDS and DTT were removed. The effective encapsulation (EE) and loading capacity (LC) of BBR was determined by UV-Vis analysis (Varian Ltd., Hong Kong). Calibration curve of BBR was made by measuring the absorbance of a series of standard BBR solutions. Concentration of BBR in nanoparticles was directly calculated by measuring the absorbance of the encapsulated drugs. The EE and LC were calculated as follows:

$$EE\% = W_{loaded}/W_{total} \times 100\%,$$

$$LC\% = W_{loaded}/W_{NP} \times 100\%.$$

W_{total} was the weight of total drug added when preparing BBR-NP, W_{NP} was the weight of BBR-NP, and W_{loaded} was the weight of drug wrapped in BBR-NP. The release behavior of BBR-NP was determined with dialysis method. The sample

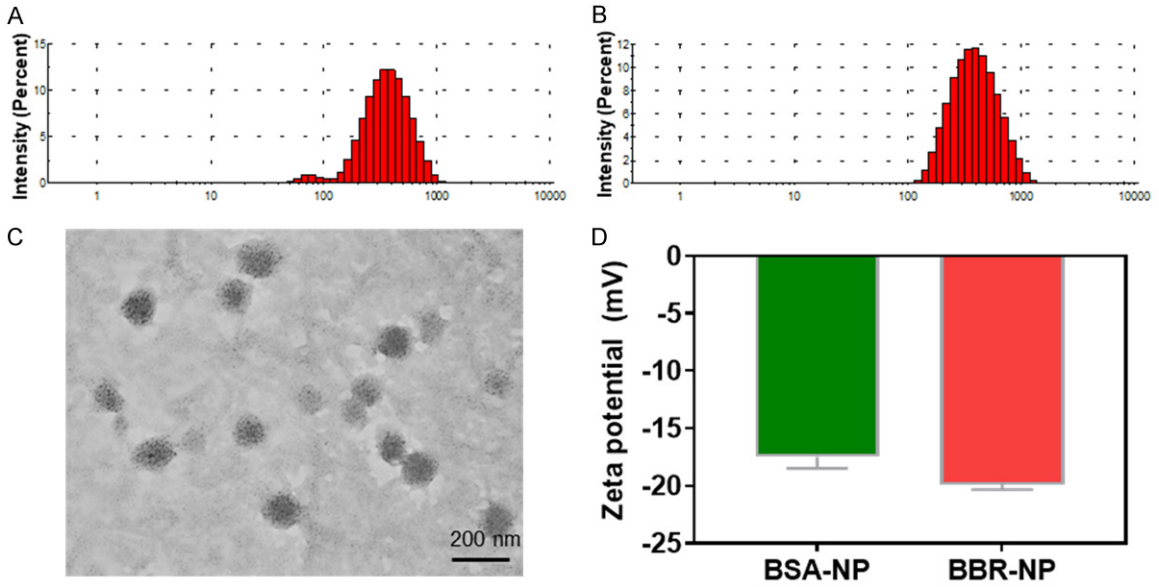

Figure 1. Preparation and characterization of BBR-NP. A. Particle size of BBR-NP (the proportion between BBR and BSA is w/w=1:5); B. Particle size of BBR-NP (w/w=1:10); C. The TEM image of BBR-NP; D. The zeta potential of BBR-NP (w/w=1:10).

containing of BBR-NP were dialyzed in a phosphate buffer saline (pH 5.5 and pH 7.4), BBR after dialysis was measured at different time points by UV-Vis at 345 nm.

$$BBR\ Release\% = M_{BBR\ release}/M_{BBR\ total} \times 100\%$$

($M_{BBR\ release}$ is the amount of BBR released from the BBR-NP at different time and $M_{BBR\ total}$ is the amount of loaded BBR).

Evaluation of the stabilizing forces of BBR-NP

To elucidate the stabilizing forces involved in the nanostructure, BSA-NP were treated with SDS (1% [wt/vol]), DTT (30 mM), Urea (2 M), which destroy hydrophobic interaction, disulfide bonds, hydrogen bond respectively. The forces for stabilizing BSA-NP were determined by DLS. To explore BBR-NP stability, the long-term stability and serum stability of nanoparticles were analyzed. BBR-NP was placed at 4°C for 60 days or 10% fetal bovine serum (FBS), the stability of nanoparticles was determined by DLS.

Against S.aureus activity of BBR-NP

The activity of BBR-NP against *S.aureus* was evaluated through the minimum inhibitory concentration (MIC) assay test. Briefly, the initial concentration of bacteria suspension in LB Broth Powder (pH 5, 6, 7) was adjusted to 1 × 10^3 CFU/mL, and the BBR and BBR-NP were diluted gradient in 96-well microplates, and microplates incubated at 37°C for 24 h. In the MIC assay, the result of Vancomycin (VA) against the strain was 0.5 μg/mL, which was in line with the standard.

Statistical analysis

All experiments were repeated at least three times unless otherwise specified. All values in the present study are presented as mean ± SD. The results were analyzed by two-tailed Student's t-test. The level of significance was set as follow: $^{*}P<0.05$; $^{**}P<0.01$; $^{***}P<0.001$. Statistical significance of the results was judged at $P<0.05$. The result was judged a higher or extremely significant difference at $P<0.01$, $P<0.001$. Asterisks are used in Figures to indicate *P*-value.

Results

Preparation and characterization of BBR-NP

The stable nanoparticles were prepared based on the adjustment of proportion between BBR and BSA (w/w from 1:1 to 1:10). Results show that when the w/w is 1:1 and 1:2, the precipitation occurred. While the w/w is 1:5 or 1:10, the nanoparticles formed. The **Figure 1A** and **1B** showed the particle size distribution of BBR-NP formed by mixing BBR and BSA, indicating the

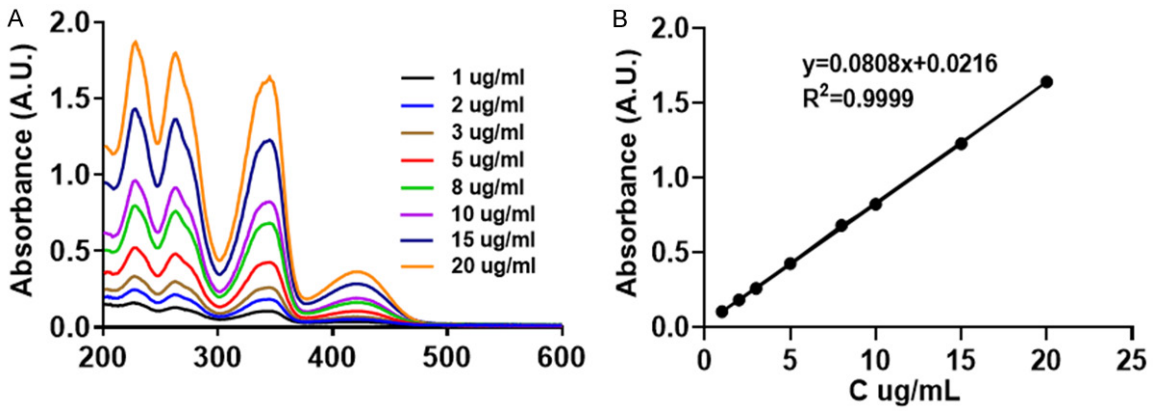

Figure 2. Studies on UV-vis spectroscopy. A. The absorption peak of BBR; B. The standard curve of BBR at 345 nm.

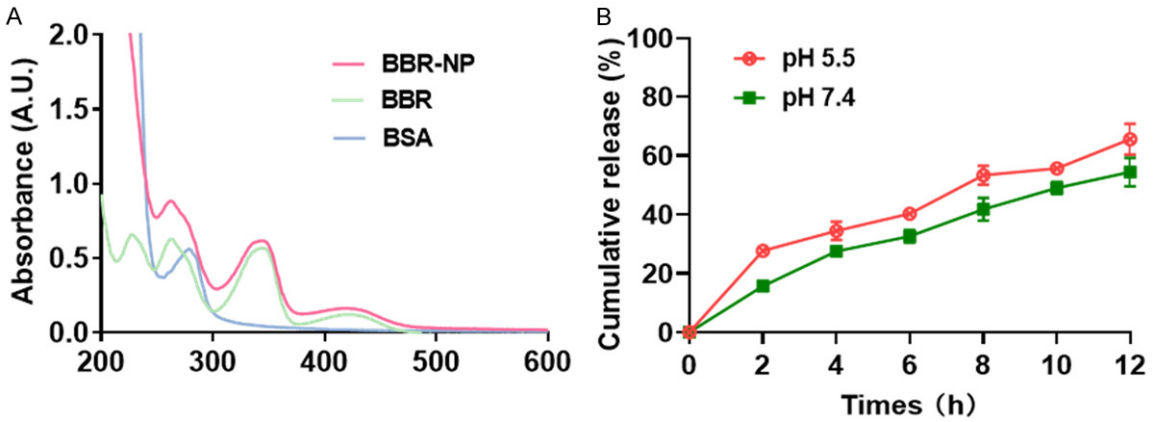

Figure 3. Studies on UV-vis of BBR-NP and release. A. The absorption peak of BBR, BBR-NP, BSA; B. The percentage of in vitro BBR released from BBR-NP in pH 5.5 and 7.4 PBS buffer.

particle size distribution of BBR-NP was narrower when the w/w is 1:10. Besides, we used transmission electron microscopy (TEM) imaging to explore the morphological characteristic of BBR-NP, and the images show that the shape of the BBR-NP is well-dispersed spherical with average size less than 150 nm (**Figure 1C**). The zeta potential of BBR-NP (w/w=1:10) decreased from -16.8 mV to -19.6 mV after adding BBR (**Figure 1D**).

Studies on UV-vis spectroscopy and release

The content of BBR within the nanoparticles could be proved by using UV-vis spectroscopy technique after removing free drugs. The results of the effective encapsulation and loading capacity of BBR encapsulated into nanoparticles were 67.0% and 3.91%, respectively (**Figures 2A**, **2B** and **3A**). The in vitro release profiles of BBR from BBR-NP were carried out in PBS at pH 5.5 and 7.4 for different time. The **Figure 3B** showed the BBR release profile was higher at pH 5.5 and reached 69% at 12 h, while pH is 7.4, the maximum releasing of BBR was about 51% at 12 h, indicating the BBR release is more conducive in acidic environment.

The stability and stabilizing forces of BBR-NP

The stability of BBR-NP was determined by binding force and size change in medium. In order to avoid coagulation or gelation caused by nanoparticles in vivo, it is essential to analyze the stability of BBR-NP in a simulated physiological environment. BBR-NP was treated with FBS (10%) at room temperature for 24 h. Also, BBR-NP was kept at 4°C for 60 days for determining long term stability. The results of **Figure 4A** and **4B** showed that BBR-NP has no significant size change, indicating they had

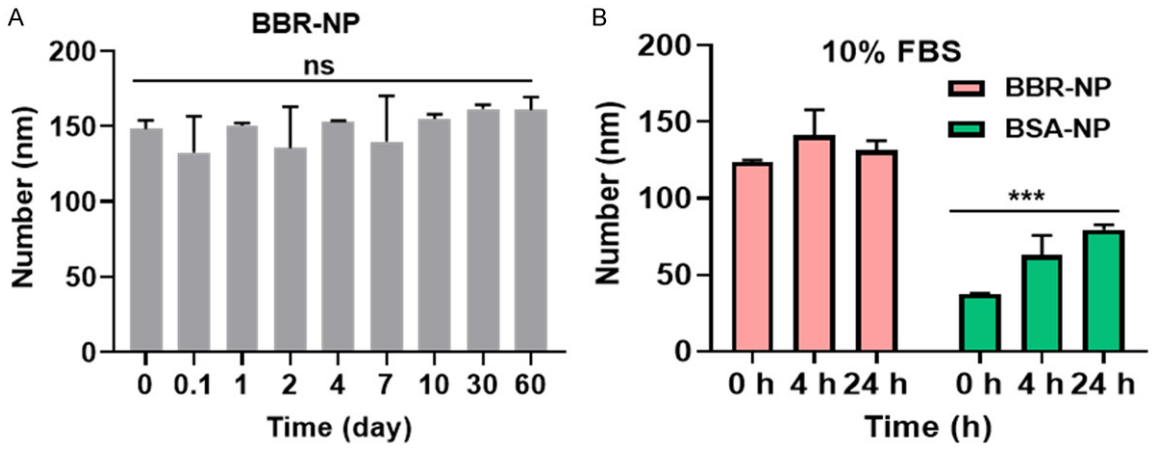

Figure 4. The stability and stabilizing forces of BBR-NP. A. Long-term stability analysis of BBR-NP by size change determination for 60 days; B. Stability analysis of BBR-NP in 10% FBS (***P<0.001).

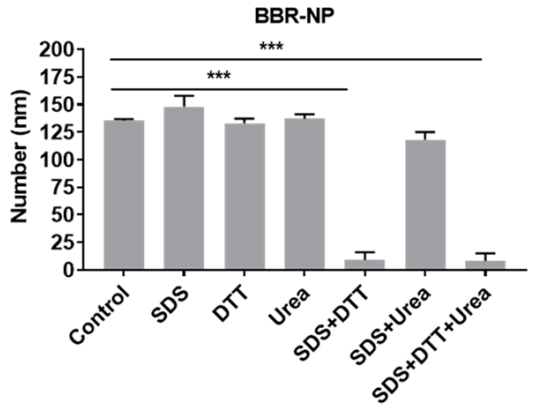

Figure 5. Effect of SDS, DTT and Urea on the size of BBR-NP. 1 to 7 are Control, SDS, DTT, Urea, SDS+DTT, SDS+Urea, SDS+DTT+Urea, respectively (***P<0.001).

excellent biological stability. The spatial binding effect has been explained with change of size. As shown in **Figure 5**, separate treatment group showed a very weak change size of BSA-NP, particularly treated with urea alone. In contrast, BSA-NP is dissociated into monomer molecules only after SDS and DTT treatment. Therefore, the dissociation behavior with the treatment of SDS and DTT is similar to SDS, DTT and Urea, which gave further evidence of the internal stability of nanoparticles through disulfide bond and hydrophobic action.

Against S.aureus activity of BBR-NP

BBR-NP at 5 μg/mL had stronger antibacterial effect in acidic environment (pH=5), while the antibacterial effect of BBR can be achieved when the BBR concentration is 200 μg/mL. It is possible that the good solubility and dispersibility makes its MIC value lower than BBR (**Table 1**). The results suggest that BBR nanoparticles may play an important role in wound infection in the future.

Table 1. The MIC of BBR and BBR-NP against *S.aureus*

pH	BBR (μg/mL)	BBR-NP (μg/mL)	VA (μg/mL)
5	200	5	0.5
6	200	20	0.25
7	100	40	0.5

Discussion

When individual immunity is impaired, patients may become vulnerable to microorganisms, resulting in an increase in the incidence of infections every year. Wound infection is the most common and serious problem after traumatic injury, and most of the pathogens of chronic wound infection were Staphylococcus Aureus and Pseudomonas Aeruginosa. The existing antibiotics are limited in effectiveness and safety, and widespread use of antibiotics leads to increasing bacterial resistance, therefore, searching for new broad-spectrum of antimicrobial agents to combat bacterial infections is urgent.

Medicinal plants are one of the potential sources of antibiotics. Berberine has been found to have synergistic anti-infective effect, but it cannot be used alone as an anti-infective drug

because of its low bioavailability in vivo. We have designed and used a safe nanocarrier based on BSA, which is a natural and biodegradable material. Our design concept is based on the hydrophobic drugs could be stabilized in the albumin disulfide bond network. For BSA, one free thiol in each BSA molecule not enough to ensure sufficient intermolecular cross-linking to form a network at the nanoscale [25, 26]. Therefore, protein is denaturated to liberate the free thiols, we assemble molecular BSA into large-sized nanostructures through the reconstructed intermolecular disulfide bond and hydrophobic interaction, and berberine with poor water solubility was encapsulated in it to afford biocompatibility and biodispersibility. BSA gradually formed nanoclusters during the assembly process, the stable nanoparticles were prepared based on the adjustment of proportion between BBR and BSA. The stability analysis demonstrated that nanoclusters were mainly stabilized with hydrophobic interactions and disulfide bonds since SDS (destroyer of hydrophobic interactions) and DTT (destroyer of disulfide bond) could lead to fast disassembly. It is reported that polymeric nanoparticles may bring about coagulation or gelation in vivo [26]. While the size distribution of BBR-NP showed slight variation after 24 h in 10% FBS, implying the more stable property of nanoparticles loaded with BBR.

The infected micro-environment is acidic due to metabolic activities of bacteria [1, 27]. Such as *S.aureus* secretes lactic acid during its growth, BBR-NP is pH-sensitive nanogels with controlled release in acidic environment. Nanoassembly with BSA markedly improved the dispersibility of BBR, making a possible to enhance its anti-infective activity. Berberine has a weak anti-bacterial effect, while the nanoparticles modified with BSA have significant antibacterial activity in acidic environment. It is more beneficial to the drug release of BBR-NP in acidic environment. We conclude that BBR-NP is the good solubility and dispersibility allows it has lower MIC value compared to BBR.

Conclusion

BBR self-assembles into nanoparticle (BBR-NP) with rBSA in vitro, which were mainly controlled by the reconstructed intermolecular disulfide bond and hydrophobic interaction. We studied the biological stability, release and antibacterial effect. The better biostability and slow-releasing suggested that the BBR-NP could serve as a promising anti-infection lead compound for further research. The MICs results show that antibacterial effect of BBR-NP is 40 times than BBR, and make it possible that BBR nanoparticles may offer new options as anti-bacterial in traumatic wounds.

Acknowledgements

This study was sponsored by Shanghai Sailing Program (21YF1436300), National Natural Science Foundation of China (82002122), Shanghai Natural Fund (21ZR1457300).

Disclosure of conflict of interest

None.

Address correspondence to: Yanhong Wang, Heilongjiang University of Chinese Medicine, No. 24 Heping Road, Xiangfang District, Harbin 150040, Heilongjiang Province, China. Tel: +86-0451-8219-3029; E-mail: 799378826@qq.com; Ning Ma, Department of Clinical Laboratory, 905th Hospital of PLA, Shanghai 200052, China. Tel: +86-0451-82193029; E-mail: mamimg@sina.com

References

[1] Wuthisuthimethawee P, Lindquist SJ, Sandler N, Clavisi O, Korin S, Watters D and Gruen RL. Wound management in disaster settings. World J Surg 2015; 39: 842-53.

[2] Perfect JR. The antifungal pipeline: a reality check. Nat Rev Drug Discov 2017; 16: 603-616.

[3] Carvalho A, Cunha C, Bozza S, Moretti S, Massi-Benedetti C, Bistoni F, Aversa F and Romani L. Immunity and tolerance to fungi in hematopoietic transplantation: principles and perspectives. Front Immunol 2012; 3: 156.

[4] LeibundGut-Landmann S, Wuthrich M and Hohl TM. Immunity to fungi. Curr Opin Immunol 2012; 24: 449-58.

[5] Älgå A, Wong S, Shoaib M, Lundgren K, Giske CG, von Schreeb J and Malmstedt J. Infection with high proportion of multidrug-resistant bacteria in conflict-related injuries is associated with poor outcomes and excess resource consumption: a cohort study of Syrian patients treated in Jordan. BMC Infect Dis 2018; 18: 233.

[6] Lloyd BA, Murray CK, Bradley W, Shaikh F, Aggarwal D, Carson ML and Tribble DR. Variation in postinjury antibiotic prophylaxis patterns over five years in a combat zone. Mil Med 2017; 182: 346-352.

[7] Malone M, Bjarnsholt T, McBain AJ, James GA, Stoodley P, Leaper D, Tachi M, Schultz G, Swanson T and Wolcott RD. The prevalence of biofilms in chronic wounds: a systematic review and meta-analysis of published data. J Wound Care 2017; 26: 20-25.

[8] Sari S, Kart D, Öztürk N, Kaynak FB, Gencel M, Taskor G, Karakurt A, Saraç S, Eşsiz Ş and Dalkara S. Discovery of new azoles with potent activity against Candida spp. and Candida albicans biofilms through virtual screening. Eur J Med Chem 2019; 179: 634-648.

[9] Feng W, Yang J, Wang Y, Chen J, Xi Z and Qiao Z. ERG11 mutations and upregulation in clinical itraconazole-resistant isolates of Candida krusei. Can J Microbiol 2016; 62: 938-943.

[10] Mukherjee PK, Chandra J, Kuhn DM and Ghannoum MA. Mechanism of fluconazole resistance in Candida albicans biofilms: phase-specific role of efflux pumps and membrane sterols. Infect Immun 2003; 71: 4333-40.

[11] Shang XF, Yang CJ, Morris-Natschke SL, Li JC, Yin XD, Liu YQ, Guo X, Peng JW, Goto M, Zhang JY and Lee KH. Biologically active isoquinoline alkaloids covering 2014-2018. Med Res Rev 2020; 40: 2212-2289.

[12] Wang J, Wang L, Lou GH, Zeng HR, Hu J, Huang QW, Peng W and Yang XB. Coptidis Rhizoma: a comprehensive review of its traditional uses, botany, phytochemistry, pharmacology and toxicology. Pharm Biol 2019; 57: 193-225.

[13] Zhang W, Hu JF, Lv WW, Zhao QC and Shi GB. Antibacterial, antifungal and cytotoxic isoquinoline alkaloids from Litsea cubeba. Molecules 2012; 17: 12950-60.

[14] Tsai IL, Liou YF and Lu ST. Screening of isoquinoline alkaloids and their derivatives for antibacterial and antifungal activities. Gaoxiong Yi Xue Ke Xue Za Zhi 1989; 5: 132-45.

[15] Ryu CK, Oh SY, Choi SJ and Kang DY. Synthesis of antifungal evaluation of 2H-[1,2,3] Triazolo[4,5-g]isoquinoline-4,9-diones. Chem Pharm Bull (Tokyo) 2014; 62: 1119-24.

[16] Divya K, Smitha V and Jisha MS. Antifungal, antioxidant and cytotoxic activities of chitosan nanoparticles and its use as an edible coating on vegetables. Int J Biol Macromol 2018; 114: 572-577.

[17] Neqal M, Fernandez J, Coma V, Gauthier M and Heroguez V. pH-Triggered release of an antifungal agent from polyglycidol-based nanoparticles against fuel fungus H. resinae. J Colloid Interface Sci 2018; 526: 135-144.

[18] Zhang M, Hagan CT 4th, Min Y, Foley H, Tian X, Yang F, Mi Y, Au KM, Medik Y, Roche K, Wagner K, Rodgers Z and Wang AZ. Nanoparticle co-delivery of wortmannin and cisplatin synergistically enhances chemoradiotherapy and reverses platinum resistance in ovarian cancer models. Biomaterials 2018; 169: 1-10.

[19] Montero N, Perez E, Benito M, Teijon C, Teijon JM, Olmo R and Blanco MD. Biocompatibility studies of intravenously administered ionic-crosslinked chitosan-BSA nanoparticles as vehicles for antitumour drugs. Int J Pharm 2019; 554: 337-351.

[20] Bi X, Su H, Shi W, Liu X, He Z, Zhang X, Sun Y and Ge D. BSA-modified poly(pyrrole-3-carboxylic acid) nanoparticles as carriers for combined chemo-photothermal therapy. J Mater Chem B 2018; 6: 7877-7888.

[21] Wen Y, Zhang W, Gong N, Wang YF, Guo HB, Guo W, Wang PC and Liang XJ. Carrier-free, self-assembled pure drug nanorods composed of 10-hydroxycamptothecin and chlorin e6 for combinatorial chemo-photodynamic antitumor therapy in vivo. Nanoscale 2017; 9: 14347-14356.

[22] Wang DL, Yu CY, Xu L, Shi LL, Tong GS, Wu JL, Liu H, Yan DY and Zhu XY. Nucleoside analogue-based supramolecular nanodrugs driven by molecular recognition for synergistic cancer therapy. J Am Chem Soc 2018; 140: 8797-8806.

[23] Wen Y, Dong H, Wang K, Li Y and Li Y. Self-templated, green-synthetic, size-controlled protein nanoassembly as a robust nanoplatform for biomedical application. ACS Appl Mater Interfaces 2018; 10: 11457-11466.

[24] Liu Y, Han Y, Fang T, Chen SM, Hu X, Song L, Shen H, Dong H, Jiang YY, Zou Z, Li Y and An MM. Turning weakness into strength: albumin nanoparticle-redirected amphotericin B biodistribution for reducing nephrotoxicity and enhancing antifungal activity. J Control Release 2020; 324: 657-668.

[25] Ruan Q, Chen Y, Kong X and Hua Y. Heat-induced aggregation and sulphydryl/disulphide reaction products of soy protein with different sulphydryl contents. Food Chem 2014; 156: 14-22.

[26] Qiu L, Hu Q, Cheng L, Li L, Tian C, Chen W, Chen Q, Hu W, Xu L, Yang J, Cheng L and Chen D. cRGDyK modified pH responsive nanoparticles for specific intracellular delivery of doxorubicin. Acta Biomater 2016; 30: 285-298.

[27] Handke LD, Rogers KL, Olson ME, Somerville GA, Jerrells TJ, Rupp ME, Dunman PM and Fey PD. Staphylococcus epidermidis saeR is an effector of anaerobic growth and a mediator of acute inflammation. Infect Immun 2008; 76: 141-52.